BIOCELL
2005, 29(2): 195-203

ISSN 0327 - 9545
PRINTED IN ARGENTINA

Changes in crossover distribution along a quadrivalent in a man carrier of a reciprocal translocation t(11;14)

M.I. Pigozzi, R.B. Sciurano, and A.J. Solari

Centro de Investigaciones en Reproducción (CIR), Facultad de Medicina, Paraguay 2155, (1121) Buenos Aires, Argentina.

Key words: Human meiotic recombination, human meiosis, crossovers, MLH1 foci, chromosomal translocations.

ABSTRACT: A testicular biopsy from an infertile man carrying a heterozygous chromosome translocation t(11;14) was studied with synaptonemal complex analysis and immunolocalization of the protein MLH1 for crossover detection. A full blockage of spermatogenesis at the spermatocyte stage was related to the presence of the translocation quadrivalents at pachytene. Only 2% of the quadrivalents showed full synapsis. Most of the spermatocytes showed asynaptic free ends that frequently mingled with the XY pair. The average number of crossovers per cell was diminished from a mean of 52.7 in controls to a mean of 48 in the patient. The difference between the number of crossovers in the quadrivalent and the normal bivalents was highly significant. The distribution of crossovers over the segment of the quadrivalent corresponding to bivalent #14 was also very different from that of the control. It is concluded that in this translocation, the pattern of crossovers is changed, mainly due to a synaptic hindrance in the quadrivalent, and that the spermatogenesis arrest is mainly due to the quadrivalents that interact with the XY pair.

Introduction

Chromosome rearrangements are known to affect the frequency and distribution of crossovers in a number of organisms (Hewitt and John, 1965). The extent and type of these changes in recombination patterns are variable among organisms. Among mammals, a net decrease in recombination has been shown in mice carriers of Robertsonian translocations (Dumas and Britton-Davidian, 2002) and increased chiasma frequencies have been found in the rearranged chromosomes of mice heterozygotes for varying reciprocal translocations (Borodin *et al.*, 1991). In human spermatocytes, reciprocal translocations can affect chiasma frequency and distribution in the involved chromosomes, as shown by chiasma analysis in metaphase I compared to normal bivalents (Armstrong *et al*., 2000; Goldman and Hulten, 1993; Laurie *et al.*, 1984 and references therein). These studies established that the number of chiasmata can be decreased or increased, and also that the distribution can be altered compared to that in the normal bivalent. A general mechanism underlying these recombinational changes has not been proved, although disturbances in homologous recognition have been suggested (Laurie *et al*., 1984).

In the mentioned studies of human spermatocytes, crossovers were scored counting chiasmata during metaphase I, a method that is useful only in those cases when high numbers of spermatocytes proceed through the meiotic division up to this stage. However, most reciprocal translocations cause a severe impairment of human spermatogenesis in heterozygotes, often with high numbers of spermatocytes being arrested at pachytene (Speed, 1989; Solari, 1999). The introduction of immunolabeling with anti-MLH1 (Baker *et al*., 1996) provides a convenient method of recording the recombination events on synaptonemal complexes during pachytene in human spermatocytes (Barlow and

Address correspondence to: Dr. Alberto J. Solari. Centro de Investigaciones en Reproducción (CIR), Facultad de Medicina, UBA, Paraguay 2155, (1121) Buenos Aires, ARGENTINA.
Tel./Fax: (+54-11) 4961-2763. E-mail: asolari@fmed.uba.ar / ajsolari@mail.retina.ar
Received on March 18, 2005. Accepted on April 11, 2005.

Hulten, 1998), facilitating the analysis of crossing over in those cases where most spermatocytes do not reach metaphase I. Additionally, the ultrastructure of a multivalent can be analyzed in detail using electron microscopy to determine the extent of synapsis.

In this paper, a reciprocal, balanced translocation between chromosomes #11 and #14 has been studied both with electron microscopy and immunolabeling for MLH1 foci, showing a decrease in the number of recombination events in the quadrivalent and striking changes in the distribution of foci along some of the elements forming the quadrivalent. The number and distribution of foci in the translocated and non-translocated segments of the quadrivalent are presented and compared to similar data in the corresponding segments of the bivalents from spermatocytes with normal karyotype, showing a significant difference between the two samples.

Materials and methods

Case

The patient PM, was referred to an andrology clinic because of infertility. A karyotype study determined a reciprocal translocation t(11;14) (q:q). A testicular biopsy was performed after informed consent of the patient and a piece of the biopsy was provided by Dr. G. Rey Valzacchi for research. This research was approved by an independent committee (CIEI). Histological analysis of the biopsy showed spermatogenesis arrest at the spermatocyte stage.

Control

Spread spermatocytes of one karyotypically normal male were used as a control for MLH1 focus analysis in bivalents #11 and #14. The identification of these bivalents was based in relative SC length and centromeric index, and their comparison with data from the literature (see Results for further details).

SC spreads and immunostaining

Part of the biopsy was used to prepare synaptonemal complex (SC) spreads on plastic-covered slides for EM according to Solari (1998) or using a drying-down method for immunostaining (Peters *et al*., 1997). The primary antibodies were: 1) a mouse monoclonal antibody against human MLH1 (Pharmingen) diluted 1:100; 2) rabbit anti-SCP3 (COR1) used at a dilution of 1:300, for use in control samples; 3) a rabbit antibody against SCP1 (Syn1) used at a dilution of 1:500; and 4) human CREST serum that binds to kinetochores. The secondary antibodies were FITC-labeled goat anti-mouse, Texas Red-labeled goat anti-human and Texas Red-labeled goat anti-rabbit. The SCs and the kinetochores give both red fluorescence, but the kinetochores on human SCs give large, distinctive signals that allow their identification. Slides were counterstained with DAPI and mounted in glycerol with antifade. Spreads were examined with a Leica fluorescence microscope and photographed with Kodak color film. Two exposures were done sequentially on the same frame: one using the FITC-filter set to capture MLH1 foci, and the second with the Texas Red set to capture SCs and centromeres. Previous tests gave no differences between this method and the superimposition of separate images regarding the numbers of MLH1 foci.

Measurements and statistical analysis

Measurements were done on digitalized images using the program MicroMeasure 3.01 (available at http://www.colostate.edu/Depts/Biology/). This program gives SC lengths, centromeric indexes and the relative and absolute distances from each MLH1 focus to the centromere. To build the histograms of MLH1 foci for each segment of the quadrivalent, focus positions were scored as relative distances from the centromere of each translocated element and then multiplied by the mean absolute length of the corresponding axis in the whole sample of nuclei, to obtain a weighed absolute distance to the centromere. This procedure compensates for variations in the absolute SC lengths in different nuclei. Statistical analyses were performed using commercially available software (Statistica, 1999 edition; Statsoft Inc.) and graphs were done in Excel. Comparisons of MLH1 foci locations in the quadrivalent and the normal bivalents were done using the Kolmogorov-Smirnov two-sample test, that measures the maximum difference between the cumulative distributions of two samples giving the probability that the observed differences have arisen by chance. Statistical analysis of the total frequencies of foci in the quadrivalent versus the two normal bivalents 11 and 14 was performed by measuring in each control cell the addition of foci in bivalent 14 plus those in bivalent 11, that, is considering the two bivalents as a single sampling space, which corresponds actually to a quadrivalent in the patient's cells. The data matrix of control versus cuadrivalents was analysed with a *t*-test.

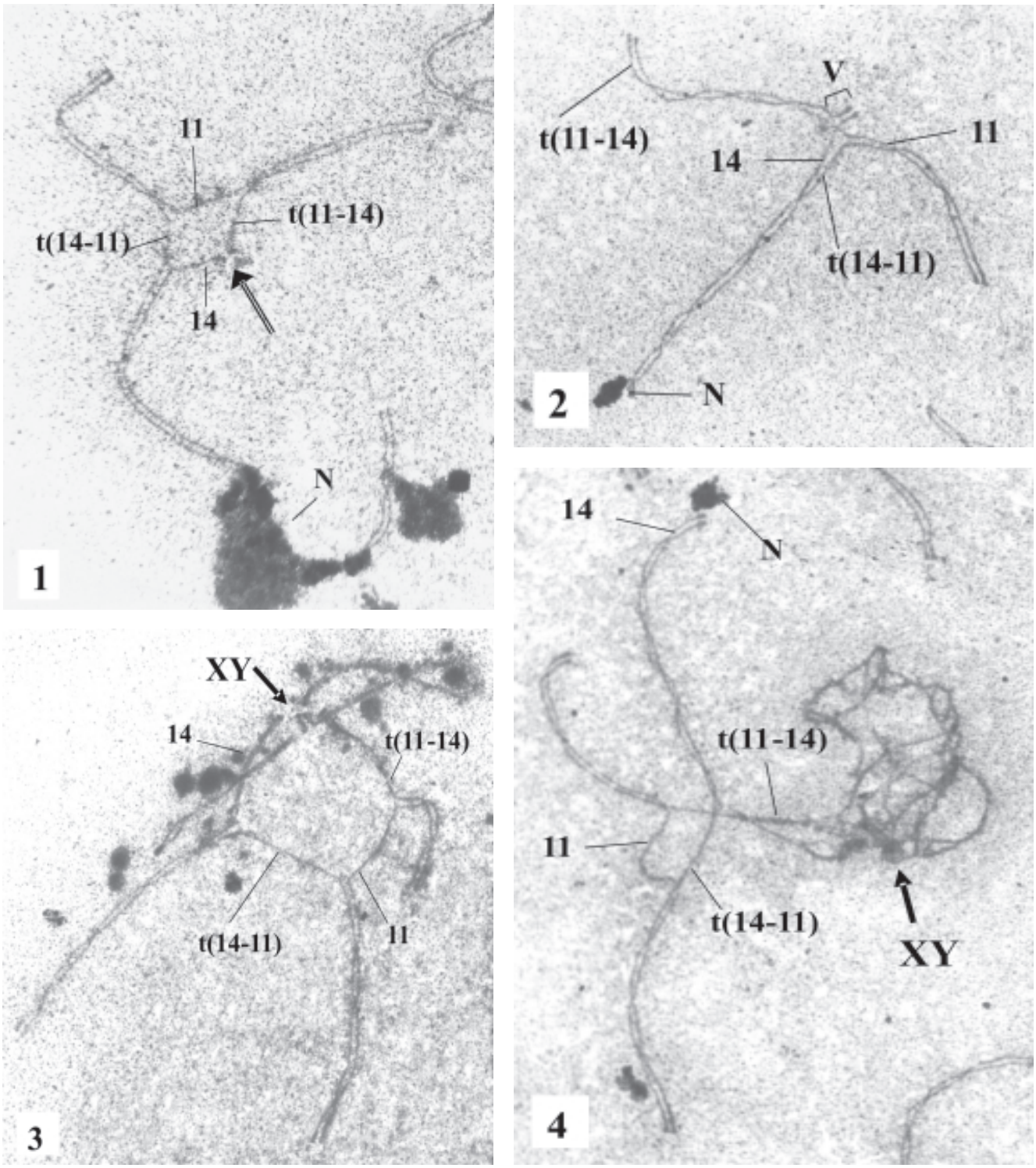

FIGURES 1-4. Electron micrographs of silver-stained quadrivalents of spread spermatocytes from the carrier of the translocation t(11;14). In **Figure 1** the four elements of the quadrivalent stand out in the typical configuration, in which the ends of #14 and the axis t(11;14) form free, asynaptic ends (arrow). N: nucleolus attached to #14p. **Figure 2** shows the rare (2% of total cells) configuration in which the quadrivalent shows full synapsis, including the "free ends" or region V. **Figure 3** shows the interaction of the "free ends" of the quadrivalent with the XY pair. The two free ends of #14 and the t(11;14) axis overlap the X and Y axes and are thickened. **Figure 4** shows a later stage of the interaction between the XY pair and the two axes having the free ends, which have become tangled within the XY body. In figures 1, 3 and 4 the quadrivalent shows asynapsis at its central region ("cross") at a place in which the axes switch partners or continue with the free ends. Magnification: X 5,000.

Results

Histology

In the translocation heterozygote the semithin (0.5 μm in thickness) sections showed spermatogenesis arrest at the spermatocyte stage, with spermatocyte apoptosis or necrosis at stages later than mid-pachytene, and a few spermatocytes that reached meiotic division and then entered in necrosis, thus confirming the diagnosis made on paraffin sections of the full testicular biopsy (not shown).

Electron microscopy

Microspread nuclei showed a typical quadrivalent formed by an acrocentric #14, a submetacentric #11 and the two translocation products: a long abnormal acrocentric and a metacentric element (Fig. 1). According to measurements on electron micrographs, the breakage points of the translocated products are: in #14q32, and in 11q13. The synaptic pattern shows a largely synapsed #14, except at the distal tip of the long arm, and a virtual full synapsis of 11q with the homologous segment translocated to 14q. (Fig. 1). In agreement with light microscopy, the tips of #14q and that of the derived #11p remain as free ends in the vast majority of cells (Fig. 1). In the samples examined with electron microscopy, only two spermatocytes over the 85 cells examined showed total synapsis along the quadrivalent, including the ends that appear generally as free ends (Fig. 2).

In a significant (20%) part of cells studied with electron microscopy, the free ends of the quadrivalent engaged in a close relationship with the XY pair (Figs. 3 and 4). In these cells the quadrivalent showed additional abnormalities, as synapsis was restricted in the axial regions close to the free termini, some axial regions were stretched and one or both of the free termini were often mingled with the axes of the XY body.

MLH1 foci in the control

Spermatocytes from the control male showed 22 autosomal bivalents and the XY pair (Fig. 5a). In a sample of 80 complete SC sets the mean number of MLH1 foci in the autosomal bivalents was 52.7 ± 3.9, ranging between 40 and 63. The number and distribution of MLH1 foci were scored in bivalent #14 in order to compare them with those of the corresponding segments in the quadrivalent. SC #14 is the acrocentric of intermediate length in group D both in mitotic and SC karyotypes, and its SC shows little variation with its expected relative length according to the mitotic karyotype (Sun *et al.*, 2004). Thus, the acrocentric SC of intermediate size was considered pair 14 in every nucleus of our analysis. The mean number of foci on SC #14 was 1.9 ± 0.4, with most SCs showing two foci: one proximal and one on distal position.

The identification of SC #11 was considered less certain because the identification of each SC in this group (based on relative length) may be ambiguous in some cells. However, when the centromeric index is used to ascertain between bivalent #11 and bivalent #12, many of these cases were defined.

MLH1 foci in the translocation heterozygote

A total of 42 spermatocytes were used for SC measurements and counting of MLH1 foci in the quadrivalent. Immunostained spermatocytes show a quadrivalent with a T-shaped configuration: two of the "arms" of the quadrivalent bear the centromeres at distinct positions, and the third arm is somewhat shorter than the other and represents most of the long arm of chromosome #11 (Fig. 5B and 5C). Because of its asymmetric constitution the predicted quadrivalent can be divided in five identifiable pairing segments to analyze the distribution of MLH1 foci (Fig. 5D). Most quadrivalents had three MLH1 foci, distributed as observed in Figure 5C, but about one third had four foci. Focus positions on segments I and III were measured as distances from the centromere of #11 (11 kc), and those on segment IV were related to the centromere of #14 (14 kc). No MLH1 foci were observed in segment V (that is asynaptic in most quadrivalents) and in segment II (that is proximal to the kinetochore of #11).

The distribution frequencies of foci in each segment are shown in figures 6A to 6C, and the distribution of foci along the normal (control) #14 is shown in Figure 6D.

Comparison between total foci in quadrivalents versus total foci in bivalents #14 and #11

In order to ascertain a variation in total crossover counts in the patient's quadrivalents as regards to the normal bivalents, 74 cells from the control (mean #11+#14 foci = 4.6) and 42 cells from the patient (mean quadrivalent foci = 3.4) were analyzed as described in Methods.

As shown in Table I, the *t*-test results show that the quadrivalent has a highly significant decrease in total foci compared to the sum of foci in normal bivalents #14 and #11.

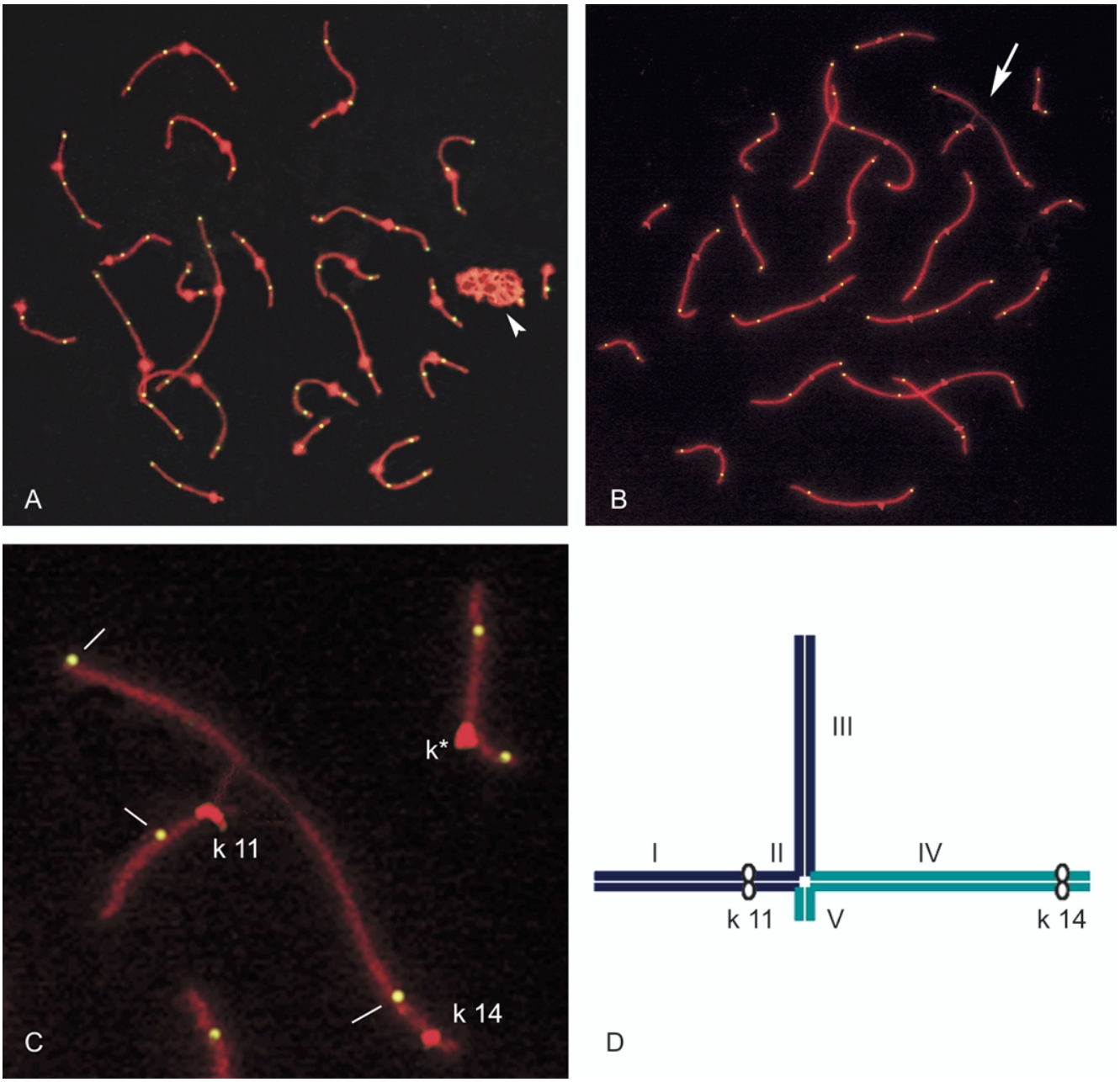

FIGURES 5A- 5D. Figures 5A-5C are light-microscope micrographs (fluorescence) of synaptonemal complex spreads with triple immunostaining. **Figure 5A** shows a control spermatocyte in which the MLH1 foci are yellow, the axes of SCs are linear red strands and kinetochores are round, red structures. The arrowhead points to the late XY pair of this cell. **Figure 5B** shows a spermatocyte from the carrier. The arrow points to the quadrivalent, which shows the three long arms and a fainter central region. MLH1 foci are yellow, the two kinetochores from #14 and #11 are round and bright red. **Figure 5C** is an enlarged part of 5B showing the quadrivalent and one autosomal bivalent at upper right. The kinetochores of #11 (center, k 11) and of #14 (lower right, k 14) stand out on the paired regions of the SCs immunostained with anti-SCP1, but the center shows only a very weak red fluorescence because this region is mainly asynaptic and holds the "free ends". **Figure 5D** shows a schematic drawing of the quadrivalent. Dark blue: regions corresponding to #11; light green, regions corresponding to #14. The "free ends" are represented as paired (region V) although pairing at this region is very rare (see Fig. 2, electron micrograph). Magnification in 5A-5B: X 1,465

TABLE I.

Comparison between the number of foci in control bivalents and the quadrivalent*

	Control [1]	Carrier [2]
Mean	4.6	3.4
SD	0.7	0.6
n	74	42

*t-value = -9.1; df = 114; p = $3.2.10^{-15}$ *very highly significant.*
[1] average of foci in the pair of bivalents #14 and #11 from the control.
[2] average of foci in quadrivalents from the carrier.

Numbers of total foci per cell

The comparison of the total number of foci in the patient's spermatocytes versus the total number of foci in control spermatocytes is depicted in Table II.

Although there is a significant decrease of the number of foci in the patient's cells, this difference has less significance than that of foci in quadrivalents versus normal bivalents (see above). Furthermore, there is about a 20% difference between the SC lengths of the patient versus that of controls.

TABLE II.

Average total number of foci per cell in the control and the carrier (and lengths of the SC sets)*

	Control [1]	Carrier [2]
Mean	52.7	48.0
SD	3.9	3.5
n	80	42

*t-value = 6.5; df = 120; p < 0.001 *highly significant.*
[1] average SC length in the control: 238.1; SD: 33.4; n: 80.
[2] average SC length in the carrier: 282.3; SD: 26.8; n: 42.

Comparison between the distribution of foci in bivalent #14 (control) with the corresponding region (IV) in the quadrivalent

The distribution of foci along the segment IV of the quadrivalent (Fig. 6A) shows a striking dissapearance of a distal peak when compared to that of the normal (control) bivalent #14 (Fig. 6D). When these two distributions were analyzed with the Kolmogorov-Smirnov test (see Methods) the test gave a statistic D = 0.245, which shows that the distributions are significantly different (p = 0.01).

Discussion

1. *Frequency and localization of crossovers in the normal human male*

There are basically two approaches to determine the number and position of crossover or recombination sites: a) by pedigree analysis and b) by cytological methods. The former has been extensively used during the making of the linkage maps of the human genome (Donnis Keller *et al.*, 1987; Broman *et al.,* 1998). The pedigree data, despite their usefulness in gene mapping and the definition of the large difference in recombination frequency between males and females (female /male ratio is about 1.6, Kong *et al.*, 2002), yields only indirect data on specific chromosome regions and is limited in accuracy for intervals <1 cM (Kong *et al*., 2002) and thus the analysis of specific sites of high recombination frequency ("hot spots") shows significant difficulties (Arnheim *et al*., 2003), although cytological methods do not generally help in this latter matter.

On the other hand, the cytological methods provide direct evidence on the number and location of recombinational events or their resulting manifestations as chiasmata, but they have the drawback of the need of performing a biopsy and their localization at a specific physical distance of chromosome markers often lacks the desirable accuracy. The cytological methods rank from the older chiasmata maps (Hulten, 1974), to the recombination nodule location in electron micrographs (Solari, 1980; Solari, 1998) and the more recent use of fluorescent immunodetection of crossovers by MLH1 detection (Baker *et al,* 1996). The frequency of crossovers in the normal human male using these different cytological methods shows a reasonable agreement – from the consensus of about 51 chiasmata (Barlow and Hulten, 1998), 46.2 recombination nodules (Solari,

1980) and the number of MLH1 foci in human spermatocytes (50.9 in Barlow and Hulten, 1998; 48 in Sun *et al*., 2005). The present results in control human spermatocytes show a mean number of MLH1 foci of 52.7, that is in close agreement with the previously cited data.

The localization of the average 50-52 crossovers over specific male meiotic bivalents through cytological methods has been a difficult task until the availability of the MLH1 immunodetection techniques, which give the opportunity to scrutinize large quantities of cells. It is now established that many individual chromosomal pairs have specific patterns of crossover location (Hulten, 1974; Solari, 1980; Fang and Jagiello, 1988; Sun *et al.*, 2004). Some general features of crossover distribution are known: a) the frequency of crossovers is grossly proportional to bivalent length or synaptonemal complex length (Rahn and Solari, 1986, in chickens; Solari, 1980 and Lynn *et al.*, 2002, in men); b) one crossover is obligatory in each autosomal bivalent. The XY pair is a special case, as - when ascertained with MLH1 foci - only about half had foci (Barlow and Hulten, 1998; 73% of the XY pairs in Sun *et al*, 2005); c) there is a strong tendency to accumulate crossovers in terminal (near-telomeric) regions of many

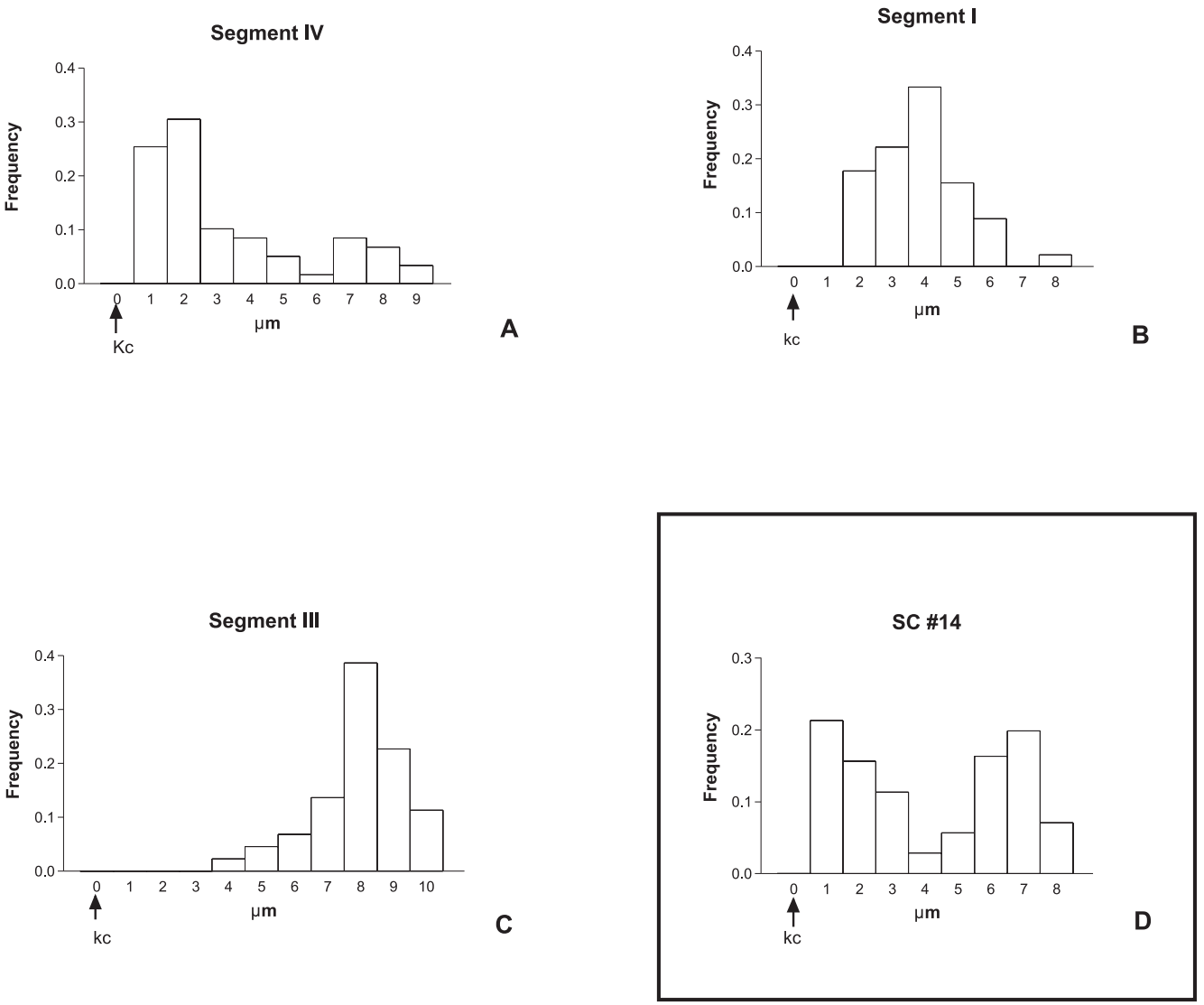

FIGURES 6A-6D. Histograms 6A, 6B and 6C show the distributions of MLH1 foci over the segments IV, I and III respectively, of the quadrivalent (see Fig. 5D). Histogram 6D shows the distribution of foci along the nomal SC #14 in the control. Histogram 6A, which corresponds to most of #14 in the quadrivalent, shows a decrease in the distal peak of foci when compared to the normal # 14 (histogram 6D).

bivalents, and a general paucity of crossovers in proximal (nearby to centromeres) regions; d) crossover interference is proved in humans (Broman and Weber, 2000; Lin *et al*, 2001).

Despite interindividual variations (Sun *et al*., 2005), these regularities allow the comparison between chiasmata location in normal bivalents and their location in cells carrying chromosomal rearrangements.

2. Disturbance of crossover number and location in rearranged chromosomes

In the present results it has been shown that identification of bivalent #14 is accurate in most spermatocytes, but the identification of #11 is somewhat uncertain by relative length only, although the addition of centromere location helps this identification. Thus, if bivalents are identified by FISH, the relative length of bivalent #11 overlaps that of bivalent #12 (Sun *et al.*, 2004) but if centromere location is added, as in the present case, most of the cells show a clear difference between both bivalents. Thus the analysis was focused on two points: a) the comparison between the total number of foci in the quadrivalent, on one side, and the sum of foci of bivalents #14 and #11 in normals; b) the comparison between the regional distribution of foci in three regions of the quadrivalent (excluding the tiny free, terminal ends) and the distribution of foci in the corresponding regions of control bivalent #14. In both cases, the statistical tests showed significant differences between the quadrivalent and the control bivalents. The present results show a highly significant total decrease of crossovers in the whole quadrivalent compared to the sum of crossovers in the normal bivalents #14 and #11. Furthermore, the regional distribution of crossovers is changed in the long arm of bivalent #14, with an almost dissapearance of the crossover peak normally located at the distal region of #14.

Both of these results may be, and probably are related to each other. The decrease of the distal peak in bivalent #14 is probably a major factor in the total decrease of crossovers in the quadrivalent. The tiny region of free terminal ends, which remains non-synapsed in the vast majority of cells, is not sufficient to originate the large decrease of crossovers at the distal #14, as it is equivalent to less than 1/5 of the total length of #14q, and the normal crossover peak at #14q stretches over 3/8 of #14q. Thus, the presence of the breakpoint and the alteration of the synaptic pattern may be related to this disturbance of crossover location.

It can be assumed that the terminal, free ends of region V are in some way delayed, and probably inhibited, in the normal meiotic pathway. A synaptic delay in this tiny region may lower the probabilities of maturing exchanges and yielding crossovers over the tiny terminal region and the preceding segments that reach synapsis, especially if that delay allows that this region reaches the threshold of the non-homologous phase of synapsis (Moses and Poorman, 1981).

Thus we assume that the disturbance of the recombination pattern is due to the steric hindrance of the organization of a functionally mature SC at the region of switching partners (the cross-center of the quadrivalent).

In a few previously published cases, contradictory results were observed in rearranged chromosomes as regards crossover location and frequency. In two men carrying different reciprocal translocations [t(9;10) and t(Y;10)] Laurie *et al.* (1984) found a local increase of chiasmata in comparison to karyotypically normal controls. However, the definition of chiasmata is notoriously more difficult than the numbering of foci, and the possibility of misinterpreting terminal, non-specific attachments by heterochromatin as chiasmata is always possible. The analysis by Goldman and Hulten (1993) of a carrier of another reciprocal translocation t(1;11), showed, on the contrary, an overall reduction of chiasmata as well as in the non-rearranged long arm of chromosome #1. The fact that actual chiasmata localizations have been made in only five men in the literature and a detailed description in only two men (reviewed in Sun *et al*., 2004) hinders any generalization. Despite that the present study is the first report – as far as we know- on the counting of foci in human chromosome rearrangements, it is reasonable to assume that rearrangements in which the multivalents show free ends, as in the present case, probably have a local decrease in crossover frequency, which stems from a local synaptic delay and final incomplete synapsis.

3. *Effects of rearrangements on spermatocyte survival and spermatogenesis completion*

The present case adds another instance of the deleterious effects of rearrangements on human spermatogenesis. As previously reviewed (Solari, 1999; Coco *et al.,* 2004) the damaging effects of rearrangements vary according to type, magnitude and complexity of the rearrangement. Thus chromosome inversions are the least damaging, and gonosome-autosome translocations nearly always lead to complete spermatogenesis blockage (Speed, 1989; Solari *et al.*, 2001). In an intermediate level of damage, the reciprocal translocations that leave free ends seem to be the more disturbing ones

(Speed, 1989; Solari, 1999). It is generally assumed that free ends are able to interact with the unpaired regions of the XY pair, and this interaction allows the spread of transcriptional inactivation from the XY body to autosomal regions, leading to spermatocyte loss. Although interchromosomal effects of rearranged chromosomes on total recombination rates have been claimed (Laurie *et al*., 1984) the present case shows only a weak evidence of such a general effect on total recombination rate and thus total crossover rates seem not to be the leading factor in spermatocyte survival and spermatogenesis completion. On the other hand, the observed frequency of interactions between the free ends and the XY pair in the present case are further evidence on the previous assumption on the origin of spermatocyte arrest, that is, the spreading of inactivation from the XY body to autosomes.

Acknowledgements

The gift of a piece of testicular biopsy from the patient and supporting clinical data from Dr. G. Rey Valzacchi are gratefully acknowledged. The research protocols are approved by the CIEI (independent committee on ethics of medical research). The helpful assistance of Lic. M.I. Rahn is gratefully acknowledged. A.S. and M.I.P. are members of the Carrera del Investigador. Financial support from UBACYT and CONICET is acknowledged.

References

Armstrong SJ, Goldman ASH, Speed RM, Hulten MA (2000). *Meiotic studies of a human male carrier of the common translocation, t(11;22), suggests postzygotic selection rather than preferential 3:1 MI segregation as the cause of liveborn offspring with an unbalanced translocation.* Am J Hum Genet 67: 601-609.

Arnheim N, Calabrese P, Nordborg M (2003). *Hot and cold spots of recombination in the human genome: the reason we should find them and how this can be achieved.* Am J Hum Genet 73: 5-16.

Baker SM, Plug AW, Prolla TA, Bronner CE, Harris AC, Yao X, Christie DM, Monell C, Arnheim N, Bradley A, Ashley T, Liskay RM (1996). *Involvement of mouse Mlh1 in DNA mismatch repair and meiotic crossing over.* Nat Genet 13: 336-342.

Barlow AL, Hulten MA (1998). *Crossing over analysis at pachytene in man.* Eur J Hum Genet 6: 350-358.

Borodin PM, Gorlov IP, Agulnik AI, Agulnik SI, Ruvinsky AO (1991). *Chromosome pairing and chiasma distribution in mice heterozygous for translocations in chromosomes 16 and 17.* Chromosoma, 101: 252-268.

Broman KW, Murray JC, Sheffield VC, White RL, Weber JL (1998). *Comprehensive human genetic maps: individual and sex-specific variation in recombination.* Am J Hum Genet 63: 861-869.

Broman KW, Weber JL (2000). *Characterization of human crossover interference.* Am J Hum Genet 66: 1911-1926.

Coco R, Rahn MI, Garcia Estanga P, Antonioli G, Solari AJ (2004). *A constitutional complex chromosome rearrangement involving meiotic arrest in an azoospermic male.* Hum Reprod 19: 2784-2790.

Donnis-Keller H, Green P, Helms C, Cartinhour S, *et al.* (1987). *A genetic linkage map of the human genome*. Cell 51: 319-337.

Dumas D, Britton-Davidian J (2002). *Chromosomal rearrangements and evolution of recombination: comparison of chiasma distribution patterns in standard and robertsonian populations of the house mouse.* Genetics 162: 1355-1366.

Fang J-S, Jagiello GM (1988). *An analysis of the chromomere map and chiasmata characteristics of human diplotene spermatocytes.* Cytogenet Cell Genet 47: 52-57.

Goldman ASH, Hulten MA (1993). *Analysis of chiasma frequency and first meiotic segregation in a human male reciprocal translocation heterozygote t(1;11) (p36.3;q13.1) using fluorescence in situ hybridization.* Cytogenet Cell Genet 63: 1623.

Hewitt GM, John B (1965). *The influence of numerical and structural chromosome mutations on chiasma conditions.* Heredity 20: 123-135.

Hulten MA (1974). *Chiasma distribution at diakinesis in the human male*. Hereditas 76: 55-78.

Kong A, Gudbjartsson DF, Sainz J, Jonsdottir GM, *et al*. (2002). *A high- resolution recombination map of the human genome.* Nat Genet 31: 241-247.

Laurie DA, Palmer RW, Hulten MA (1984). *Studies on chiasma frequency and distribution in two fertile men carrying reciprocal translocations; one with a t(9;10) karyotype and one with a t(Y;10) karyotype.* Hum Genet 68: 235-247.

Lin S, Cheng R, Wright FA (2001). *Genetic crossover interference in the human genome.* Ann Hum Genet 65: 79-93.

Lynn A, Koehler KE, Judis LA, Chan ER, *et al.* (2002). *Covariation of synaptonemal complex length and mammalian meiotic exchange rates*. Science 296: 2222-2225.

Moses MJ, Poorman PA (1981). *Synaptonemal complex analysis of mouse chromosome rearrangements.II. Synaptic adjustment in a tandem duplication.* Chromosoma 18: 519-535.

Peters A, Plug AW, Van Wugt MJ, De Boer P (1997). *A drying-down technique for the spreading of mammalian meiocytes from the male and female germline*. Chromosome Res 5: 66-71.

Rahn MI, Solari AJ (1986). *Recombination nodules in the oocytes of the chicken, Gallus domesticus*. Cytogenet Cell Genet 43: 187-193.

Speed RM (1989). *Heterologous pairing and fertility in humans*. In: Fertility and Chromosome Pairing: Recent Studies in Plants and Animals. Gillies, CB, Ed. CRC Press, Boca Raton, pp 1-35.

Solari AJ (1980). *Synaptonemal complexes and associated structures in microspread human spermatocytes.* Chromosoma 81: 315-337.

Solari AJ (1998). *Structural analysis of meiotic chromosomes and synaptonemal complexes in higher vertebrates.* In: Nuclear Structure and Function. Berrios M, (Ed). Academic Press, San Diego, pp.235-256.

Solari AJ (1999). *Synaptonemal complex analysis in human male infertility*. Eur J Histochem 43: 265-276.

Solari AJ, Rahn IM, Ferreyra ME, Carballo MA (2001*). The behavior of sex chromosomes in two human X-autosome translocation: failure of extensive X-inactivation spreading*. Biocell 25: 155-166.

Sun F, Oliver-Bonet M, Liher T, Starke H, Ko E, Rademaker A, Navarro J, Benet J, Martin RH (2004). *Human male recombination maps for individual chromosomes.* Am J Hum Genet 74: 521-531.

Sun F, Trpkov K, Rademaker A, Ko E, Martin RH (2005*). Variation in meiotic recombination frequencies among human males*. Hum Genet 116: 172-178.